5626 J. Med. Chem. 2009, 52, 5626–5634
DOI: 10.1021/jm9006577

Journal of Medicinal Chemistry Article

N-Hydroxybenzimidazole Inhibitors of the Transcription Factor LcrF in *Yersinia*: Novel Antivirulence Agents

Oak K. Kim,* Lynne K. Garrity-Ryan, Victoria J. Bartlett,† Mark C. Grier, Atul K. Verma, Gabriel Medjanis, Janice E. Donatelli, Ann B. Macone, S. Ken Tanaka, Stuart B. Levy, and Michael N. Alekshun‡

Paratek Pharmaceuticals, Inc., 75 Kneeland Street, Boston, Massachusetts 02111. †Current address: Wyeth Research, 200 Cambridge Park Drive, Cambridge, MA 02140. ‡Current address: Schering-Plough Research Institute, 2015 Galloping Hill Road, Kenilworth, NJ 07033.

Received May 18, 2009

LcrF, a multiple adaptational response (MAR) transcription factor, regulates virulence in *Yersinia pestis* and *Yersinia pseudotuberculosis*. In a search for small molecule inhibitors of LcrF, an acrylic amide series of *N*-hydroxybenzimidazoles was synthesized and the SAR (structure−activity relationship) was examined. Selected test compounds demonstrated inhibitory activity in a primary cell-free LcrF−DNA binding assay as well as in a secondary whole cell assay (type III secretion system dependent *Y. pseudotuberculosis* cytotoxicity assay). The inhibitors exhibited no measurable antibacterial activity in vitro, confirming that they do not target bacterial growth. These results demonstrate that *N*-hydroxybenzimidazole inhibitors, exemplified by **14**, **22**, and **36**, are effective antivirulence agents and have the potential to prevent infections caused by *Yersinia* spp.

Introduction

Yersinia pestis (*Y. pestis*), a Gram-negative pathogen, is the causative agent of plague[1] and poses a serious concern for its potential use as a biological weapon.[2] Clinical isolates of single- and multidrug resistant (MDR[a]) *Y. pestis* have been reported,[3] which undermines the effectiveness of current therapeutics. Therefore, with the ever-growing antimicrobial resistance problems worldwide,[4] efforts to identify new therapies for MDR *Y. pestis* infections are viewed as a pressing public health need.

Most antibiotics that have entered the market or advanced to late-stage clinical development in recent years are improved derivatives of existing chemical classes, with very few exceptions.[5,6] Such antibiotics will certainly benefit patients infected with drug resistant bacteria. However, with increasing use of new drugs, emergence of resistant strains will probably be a matter of time. The effort to identify new chemical classes of antibiotics with novel mechanisms of action through target-based high-throughput screening has not been very fruitful.[6] Clearly, circumventing bacterial resistance has proven to be a challenging task and will require more innovative research approaches.

As an alternative to traditional antimicrobial chemotherapy, strategies for targeting pathogen virulence have been reported in the recent literature.[7−9] In this regard, we have been developing small molecule anti-infection drugs that target the ability of the bacteria to cause infection (virulence) rather than growth.[10] Such antivirulence agents could be used to prevent infection of individuals in a high-risk environment such as in a bioterrorism event. The bacterial virulence targets of interest are multiple adaptational response (MAR)[11,12] transcription factors that are regulators of virulence expression.[13]

MAR proteins are characterized by two highly conserved helix−turn−helix (HTH) DNA-binding domains.[14] They are present in many clinically important Gram-negative and Gram-positive bacteria.[15] They control the ability of bacteria to cause infections, resist antibiotics, and adapt to hostile environments. Inactivation of MAR proteins by mutation attenuates the virulence of bacteria in animal models of infection but does not affect bacterial growth in vitro.[13,16−18] Thus, by design, inhibitors of MAR proteins lack inherent antimicrobial activity and are far less likely than antibiotics to apply selective pressure for the development of resistance. MAR proteins have not been described in eukaryotic cells, making this family of proteins a desirable target in antimicrobial drug discovery.

LcrF is a MAR transcription factor associated with virulence in *Y. pestis* and *Yersinia pseudotuberculosis*. It regulates expression of a type III secretion system (T3SS), a major virulence determinant of many Gram-negative bacteria (Figure 1). Upon contact with a host cell or following a change in temperature (e.g., from 26 °C in the flea to 37 °C in a human host), LcrF is expressed and then activates expression of *Yersinia* outer proteins (Yops) and the T3SS.[19] The Yops (i.e., cytotoxins) are secreted into host cells through the T3SS and result in cellular apoptosis.[20,21] Mutants that do not express the T3SS show dramatic attenuation of virulence in whole cell and animal models of infection.[22−24]

*To whom correspondence should be addressed. Phone: (617) 275-0040 (ext. 468). Fax: (617) 275-0039. E-mail: okim@paratekpharm.com.

[a] Abbreviations: MAR, multiple adaptational response; SAR, structure−activity relationship; MDR, multidrug resistance; HTH, helix−turn−helix; T3SS, type III secretion system; Yops, *Yersinia* outer proteins; LD_{50}, 50% lethal dose; CFU, colony forming unit; IC_{50}, 50% inhibitory concentration; MIC, minimum inhibitory concentration; ATCC, American Type Culture Collection; His, histidine; HRP, horseradish peroxidase; DMEM, Dulbecco's Minimal Essential Medium; LDH, lactate dehydrogenase; CLSI, Clinical and Laboratory Standards Institute.

 Published on Web 08/26/2009

Flashner et al. have recently investigated the effects of *lcrF* deletion (Δ*lcrF*) on the pathogenicity of *Y. pestis* in a mouse model of septic infection.[16] The LD_{50} (50% lethal dose) of wild-type *Y. pestis* in this model is approximately 1 colony forming unit (CFU), whereas the LD_{50} of Δ*lcrF Y. pestis* is >100 CFUs. This result demonstrates that LcrF is a valid antivirulence target in *Yersinia* spp.[25]

Small molecule compounds that inhibit the virulence of *Yersinia* are described in the literature.[26−28] These compounds are known to inhibit the type III secretion of *Yersinia*; however, their specific bacterial targets are not defined. In contrast, we aim to inhibit *Yersinia* virulence at the transcription level by targeting the LcrF protein, which in turn regulates the expression of the T3SS. Small molecule inhibitors that directly target LcrF have not been reported in the literature to date.[29]

Previously we reported *N*-hydroxybenzimidazole compounds (**1**) (Figure 2) that demonstrated inhibitory activity against the MAR proteins MarA, SoxS, and Rob in *E. coli*.[10] The *N*-hydroxybenzimidazole scaffold was initially identified from small molecule docking experiments using MarA−DNA and Rob−DNA cocrystal structures.[30,31] While the X-ray crystal structure of LcrF−DNA complex or LcrF protein has not been resolved to date, the amino acid sequence of LcrF in the DNA binding domain is known to be homologous to that of MarA, SoxS, and Rob with 31% identity and 53% similarity over a 92 amino acid stretch.[32] Therefore, initial screening of the previously identified inhibitors was viewed as a reasonable starting point in a search for LcrF inhibitors. Our goal was to identify and to develop inhibitors for LcrF−DNA binding using in vitro cell-free and whole cell assays as well as in vivo mouse models of infection caused by *Yersinia* spp.

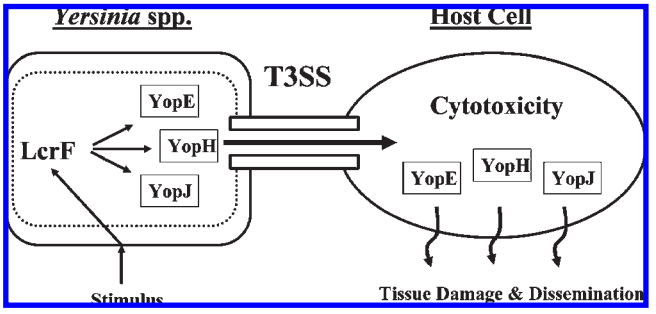

Figure 1. Diagramatic representation of Yop expression and T3SS (type III secretion system) expression in *Yersinia* spp.

Chemistry

The *N*-hydroxybenzimidazoles in the lead series were synthesized using modified literature procedures (Scheme 1).[33,34] A substituted *o*-nitro-fluorobenzene or the corresponding chloro analogue was subjected to nucleophilic aromatic substitution (S_NAr) reaction with a 4-aminobenzylamine to form 4-aminobenzyl-2-nitrophenylamine (**3**). Subsequent cyclization reaction in the presence of a base such as sodium hydride, potassium *tert*-butoxide, or sodium methoxide resulted in the formation of 2-(4-aminophenyl)-1-hydroxy-benzimidazole (**4**). When L is F or Cl, a non-nucleophilic base such as sodium hydride was used to avoid S_NAr reaction at that position (see Scheme 2). Further reaction of the cyclized intermediate **4** with an appropriate acid chloride (ca. 2.5 equiv.) in either pyridine or *N*-methylpyrrolidone generated bis-acylated product **5** (not isolated), which was then hydrolyzed in situ to afford the product **6**. Alternatively, depending on commercial availability or functional group compatibility, *N*-hydroxybenzimidazoles were also prepared starting with a substituted 4-amino benzonitrile (Scheme 2). Amide formation with an acid chloride followed by catalytic hydrogenation provided 4-phenyl acrylic amido benzylamine derivative **7**, which was then reacted with an activated nitrobenzene to give **8**. Subsequently, with the intermediate **8** (for L = F or Cl), various functional groups R_5 were introduced. For amino group

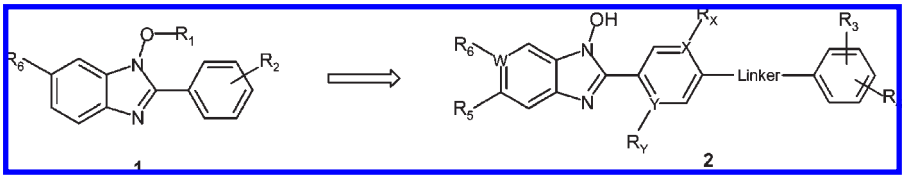

Figure 2. General structure of *N*-hydroxybenzimidazoles.

Scheme 1. Method A: General Synthesis of *N*-Hydroxybenzimidazoles

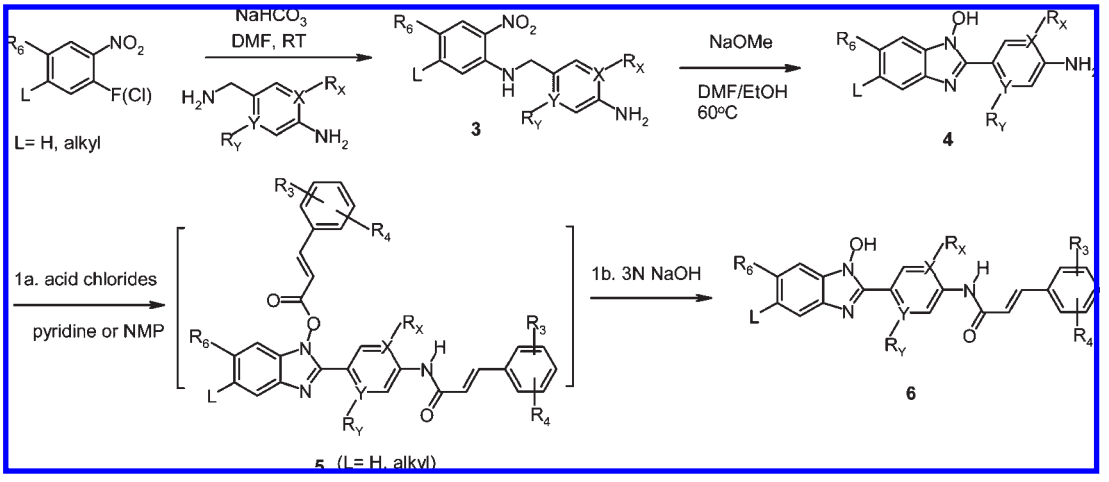

Scheme 2. Method B: Alternative Synthesis of *N*-Hydroxybenzimidazoles

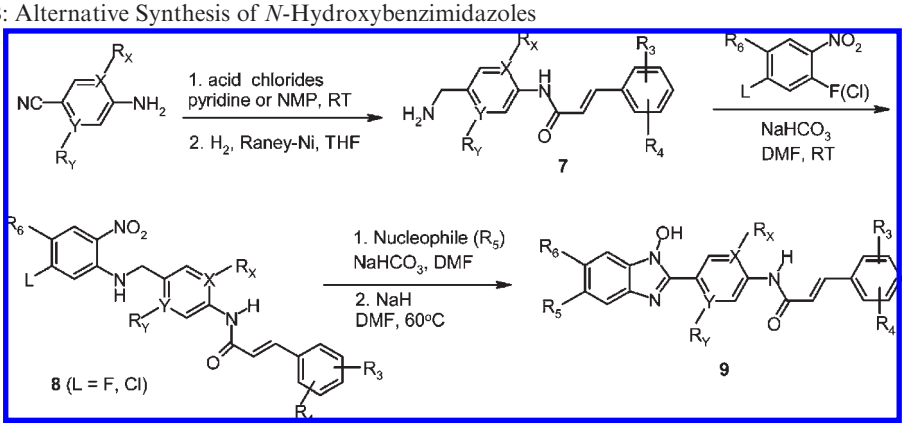

Table 1. Linker SAR of *N*-Hydroxybenzimidazoles

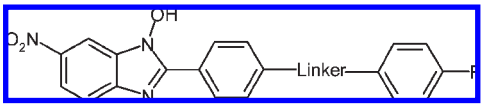

compd	linker	LcrF IC_{50} (μM)[a]
10	NHCO	17.7
11	CH_2NHCO	> 58.4
12	$NHCOCH_2$	> 58.4
13	$NHCOCH_2CH_2$	> 53.5
14	NHCOCH=CH	3.9
15	$CH_2NHCOCH$=CH	14.0

[a] IC_{50} was determined using a dose−response analysis with a maximum concentration of 25 μg/mL. Data represent the average values from two independent experiments unless specified otherwise in the Experimental Section.

substitutions at R_5, compound **8** was reacted with the corresponding amines in the presence of sodium bicarbonate and then following cyclization reaction provided **9**. For alkoxy groups at R_5, nucleophilic substitution reaction and cyclization of **8** occurred in one-pot in the presence of the corresponding alcohols (e.g., methanol, ethanol, etc.) and a base such as sodium hydride. This synthetic route proved to be highly efficient in generating R_5 substituted *N*-hydroxybenzimidazole derivatives **9**.

Results and Discussion

The inhibitory activity of *N*-hydroxybenzimidazole derivatives was measured using an in vitro cell-free LcrF−DNA binding assay and is reported as IC_{50} values (see Experimental Section).

Among the previously identified inhibitors of SoxS−DNA binding, compound **10** (Table 1) displayed good inhibitory activity for LcrF (IC_{50} = 17.7 μM). As demonstrated in our earlier communication, the lead series of inhibitors in the SoxS−DNA binding assay consisted of a *N*-hyroxybenzimidazole core with a substituted phenyl amide.[10] For the inhibition of LcrF−DNA binding, four different parts of the core structure were investigated to establish SAR: linker, terminal phenyl group (R_3/R_4), middle phenyl group (X, Y, R_X, and R_Y), and benzimidazole ring (R_5, R_6, and W) (general structure **2** in Figure 2).

To further improve the activity of **10**, a variety of different linkers were introduced between the two phenyl groups (Table 1). According to our previous work, an amide linker in **10** provided better inhibitory activity than other linkers such as amino and ether groups.[10] Therefore, in this linker SAR study, we focused on the evaluation of selected amide analogues (**11**−**15**). Extension of the amide linker in **10** with methylene groups in either direction (**11**, **12**, and **13**) resulted in derivatives with no measurable activity. Insertion of a vinyl group in compound **14** improved inhibition (IC_{50} = 3.9 μM), however, addition of another methylene group in **15** (IC_{50} = 14.0 μM) decreased activity. Within this linker series, the acrylic amide group in **14** was established as the most effective linker moiety, prompting further investigation of more substituted derivatives in acrylic amide series (Tables 2−5).

Table 2. Substitution Effect of R_3 and R_4

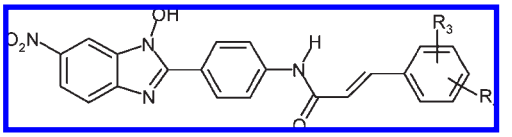

compd	R_3/R_4	LcrF IC_{50} (μM)[a]
14	4-F	3.9
16	H	6.9
17	2,4-F/F	5.0
18	3,4-F/F	14.5
19	4-CN	16.4
20	$4\text{-}CH_3$	0.8
21	$2\text{-}OCH_3$	20.9
22	$4\text{-}OCH_3$	8.0
23	$4\text{-}CF_3$	6.4
24	$2,4\text{-}OCH_3/OCH_3$	38.5
25	4-*iso*-propyl	> 50.9
26	$4\text{-}N(CH_3)_2$	16.9
27	4-1*H*-[1,2,4]triazole	35.7
28	4-1*H*-imidazole	> 44.8
29	4-OH	> 57.0

[a] IC_{50} was determined using a dose−response analysis with a maximum concentration of 25 μg/mL. Data represent the average values from two independent experiments unless specified otherwise in the Experimental Section.

In Table 2, an additional 14 compounds with varying substitutions R_3/R_4 were evaluated. Among the compounds examined, 4-H (**16**), 2,4-F/F (**17**), $4\text{-}CH_3$ (**20**), $4\text{-}OCH_3$ (**22**), and $4\text{-}CF_3$ (**23**) showed slightly improved or comparable inhibitory activity to that of **14**, whereas relatively large substitutions in **24**, **25**, **27**, and **28** resulted in loss of activity. No clear SAR emerged from the modification of R_3/R_4, however, the data in Table 2 suggest that a small lipophilic group at R_3/R_4 is a general requirement for a good inhibitor.

Table 3. Substitution Effect at the Middle Phenyl Ring

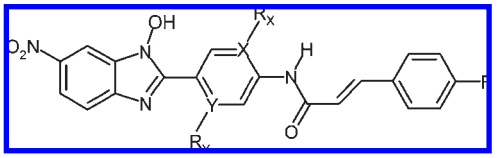

compd	X	R_X	Y	R_Y	LcrF IC_{50} (μM)[a]
14	C	H	C	H	3.9
30	N		C	H	7.4
31	C	H	N		10.8
32	C	F	C	H	20.7
33	C	H	C	F	6.5
34	C	CH_3	C	H	25.3
35	C	H	C	OCH_3	13.5

[a] IC_{50} was determined using a dose−response analysis with a maximum concentration of 25 μg/mL. Data represent the average values from two independent experiments unless specified otherwise in the Experimental Section.

Table 4. Substitution Effect of R_5

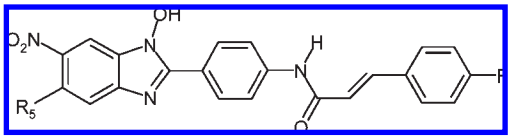

compd	R_5	LcrF IC_{50} (μM)
14	H	3.9[a]
36	CH_3	7.6[a]
37	OCH_2CH_3	17.1[a]
38	F	26.6[b]
39	$N(CH_3)_2$	66.0[b]
40	$N(CH_3)CH_2CH_2N(CH_3)_2$	3.3[c]
41	OCH_2CH_2(1-methyl-4-piperazine)	3.1[c]

[a] IC_{50} was determined using a dose−response analysis with a maximum concentration of 25 μg/mL. [b] IC_{50} determined with a maximum concentration of 50 μg/mL. [c] Nonspecific DNA binding. Data represent the average values from two independent experiments unless specified otherwise in the Experimental Section.

Further analysis of SAR in this series would be difficult without having structural information on the binding site of LcrF protein. Compound **20** showed the best inhibitory activity (IC_{50} = 0.8 μM) in this series.

In the next set of *N*-hydroxybenzimidazole derivatives, selected modifications were made at the middle phenyl ring (Table 3). Substitution of nitrogen atoms at positions X (**30**) and Y (**31**) showed comparable to slightly decreased activity over their corresponding carbon analogue **14**. While substitution of a fluorine atom at R_Y (**33**) was tolerated, the fluorine at R_X (**32**) was unfavorable for activity. Both the $-CH_3$ group at R_X (**34**) and the $-OCH_3$ group at R_Y (**35**) displayed reduced activity compared to **14**. As the SAR in Table 3 indicates, the middle phenyl ring is not likely to accommodate an extended range of substitutions.

Table 4 summarizes the substitution effect of R_5 groups. While the $-CH_3$ group in **36** maintained the activity of **14**, the $-OCH_2CH_3$ group in **37** resulted in 4-fold decrease relative to **14**. This may be linked to the increased steric effect of the $-OCH_2CH_3$ group in **37**. The substitution of $-F$ at R_5 (**38**) showed much reduced activity. Considering the relatively small size of fluorine, its electron withdrawing effect may have contributed to the weak activity of **38**. Aside from potentially unfavorable steric effect of the $-N(CH_3)_2$ group,

Table 5. Substitution Effect of R_6

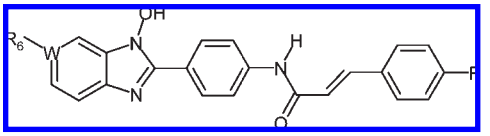

compd	W	R_6	LcrF IC_{50} (μM)
14	C	NO_2	3.9[a]
42	C	H	> 100[b]
43	N		> 54.8[a]
44	C	F	> 100[b]
45	C	CN	8.3[a]
46	C	Cl	> 100[b]
47	C	CF_3	59.7[b]
48	C	$COCH_3$	39.4[b]
49	C	SO_2CH_3	87.4[b]
50	C	1*H*-pyrazole	53.7[a]
51	C	1*H*-imidazole	37.3[a]
52	C	COOH	38.5[b]

[a] IC_{50} was determined using a dose−response analysis with a maximum concentration of 25 μg/mL. [b] IC_{50} determined with a maximum concentration of 50 μg/mL. Data represent the average values from two independent experiments unless specified otherwise in the Experimental Section.

factors contributing to the inactivity of **39** are not understood. The inhibitory activity of compound **40** is attributed to its nonspecific binding to DNA, as determined using an agarose gel electrophoresis assay (see Experimental Section), not to inhibition of LcrF−DNA binding. Given the similar basic nature of the amino group at R_5, compound **41** is likely to bind to DNA as well.

The effects of various R_6 groups are summarized in Table 5. Of the 12 R_6 groups evaluated, the $-NO_2$ group in **14** and the $-CN$ group in **45** exhibited greater inhibitory activity than the others. In the literature $-COCH_3$ and $-SO_2CH_3$ groups are described as isosteric replacements for a $-NO_2$ group,[35] whereas an imidazole group is indicated as a bioisostere of $-NO_2$ and $-CN$ groups.[36] In our *N*-hydroxybenzimidazole series, however, none of these potential isosteres (in **48**, **49**, and **51**) maintained the activity of **14**. Of the other R_6 groups, the $-COOH$ group in **52** may have similar properties (e.g., lipophilicity, molar volume, and ionizability) to those of the $-NO_2$ group in **14**. Nonetheless, compound **52** lacks inhibitory activity, presumably because of H-bonding donor ability of the $-COOH$ group.

Select compounds in the acrylic amide series ($IC_{50} \leq 25\ \mu M$) were screened using a whole cell cytotoxicity assay (inhibition of T3SS-dependent *Y. pseudotuberculosis* killing of macrophages in vitro).[37,38] As a control experiment, all compounds were tested for their intrinsic toxicity and were noncytotoxic in vitro to uninfected J774A.1 murine macrophages at a concentration of 50 μg/mL. In this assay, an *lcrF* null mutant strain (Δ*lcrF*) typically induces only 15−25% of the cytotoxicity caused by a wild-type *Y. pseudotuberculosis* (WT) (Figure 3). Among 20 test compounds, **14**, **18**, **19**, **22**, **36**, and **37** reduced *Y. pseudotuberculosis* cytotoxicity to a level approaching that of the Δ*lcrF* mutant (Figure 3). Activity (IC_{50} values) in the cell-free LcrF−DNA binding assay did not always correlate with activity in the whole cell assay. For example, compounds **19** and **31**, which exhibited similar inhibitory activity in the LcrF−DNA binding assay (IC_{50} = 16.4 and 10.8 μM, respectively), had very different activities in the whole cell assay. While compound **19** strongly inhibited

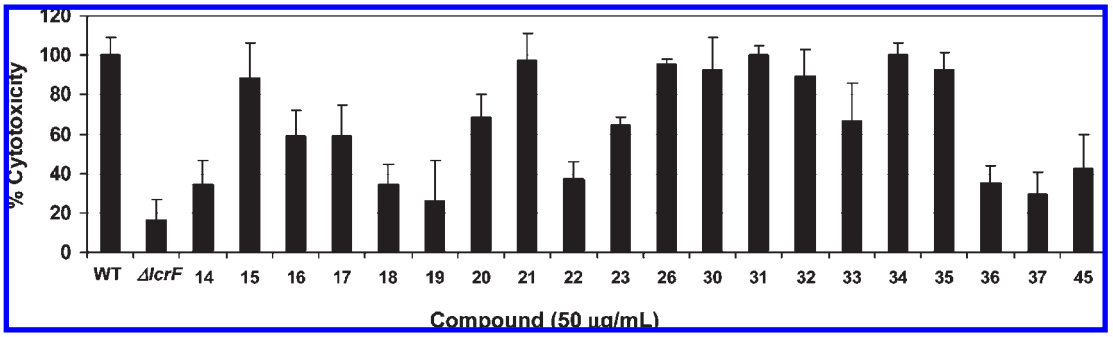

Figure 3. Inhibition of cytotoxicity caused by *Y. pseudotuberculosis* in J774A.1 cells. WT, a wild-type strain (YPIIIpIB1) of *Y. pseudotuberculosis*; Δ*lcrF*, a *lcrF* null mutant strain (YPIIIpIB1Δ*lcrF*) of *Y. pseudotuberculosis*. Data are mean values ± standard deviation with $n \geq 4$ (number of replicates).

Table 6. Target Specificity and in Vitro Antibacterial Activity

	IC_{50} (μM)[a]			MIC (μg/mL)		
compd	LcrF	ExsA[b]	SlyA[c]	*Y. pseudotuberculosis*[d]	*S. aureus*[e]	*E. coli*[f]
14	3.9	3.5	> 53.8	> 64	> 64	> 64
22	8.0	5.9	> 55.2	> 64	> 64	> 64
36	7.6	6.7	> 52	> 64	> 64	> 64

[a] IC_{50} was determined using a dose−response analysis with the maximum concentration of 25 μg/mL. Data represent the average values from two independent experiments unless specified otherwise in the Experimental Section. [b] MAR transcription factor in *P. aeruginosa*. [c] MarR family transcription factor in *Salmonella* spp. [d] YPIIIpIB1 strain of *Y. pseudotuberculosis*. [e] RN450 strain of *S. aureus*. [f] ATCC25922 strain of *E. coli*.

cytotoxicity, compound **31** was devoid of any measurable activity in the whole cell assay. Also, compound **20**, the best inhibitor (IC_{50} = 0.8 μM) identified from the LcrF−DNA binding assay, was relatively inactive in the whole cell assay. This lack of whole cell activity may have resulted from poor membrane permeability; however, variables (e.g., physicochemical parameters) that affected the permeability of compounds are not clearly understood. There may also have been undetected differences in compound solubility in the whole cell assay media, which is distinct from the media used in the LcrF−DNA binding assay (see Experimental Section). It is also possible that *N*-hydroxybenzimidazoles may exert their effects on targets other than LcrF in the whole cell assay. Overall, the results demonstrate that select compounds with good inhibitory activity against LcrF−DNA binding also effectively inhibited the virulence of *Yersinia* in the whole cell assay.

To validate target specificity, select compounds (**14**, **22**, and **36** with $IC_{50} \leq 10$ μM) were further evaluated in both ExsA−DNA and SlyA−DNA binding assays (Table 6). ExsA is a MAR transcription factor found in *Pseudomonas aeruginosa* and shares a high degree of homology with LcrF in the DNA binding domain (85% identity and 92% similarity).[32] Therefore, if these inhibitors are indeed targeting the DNA binding domain of LcrF protein, they would be likely to inhibit ExsA−DNA binding with similar potency. As shown in Table 6, all three test compounds exhibited very close IC_{50} values for both LcrF and ExsA. The DNA binding motif of SlyA, a MarR family of transcription factor in *Salmonella* spp., is different from that of MAR proteins.[39,40] Therefore, a SlyA−DNA binding assay was used to test the specificity of LcrF inhibitors. No measurable activity of the LcrF inhibitors was observed in the SlyA−DNA binding assay (Table 6). Most *N*-hydroxybenzimidazole derivatives tested in DNA binding−agarose gel electrophoresis assays displayed no detectable binding to DNA with the exception of compounds structurally related to **40** and **41**. These results confirm the target specificity of *N*-hydroxybenzimidazole inhibitors for MAR transcription factors. In an in vitro antimicrobial susceptibility test, compounds **14**, **22**, and **36** showed no measurable antibacterial activity against *Y. pseudotuberculosis* as well as *S. aureus* and *E. coli* (Table 6), verifying that they do not target bacterial growth.

Conclusions

A novel class of small molecules based on the *N*-hydroxybenzimidazole scaffold was developed as inhibitors of LcrF−DNA binding. They inhibit the virulence of *Yersinia* by targeting the LcrF protein, a MAR transcription factor. Select compounds in the acrylic amide series demonstrated inhibitory activity in a cell-free LcrF−DNA binding assay. Their antivirulence activity was further confirmed by using a T3SS-dependent whole cell assay. This class of compounds, exemplified by **14**, **22**, and **36**, is nonantibacterial, noncytotoxic, non-DNA binding, and shows specificity for MAR proteins. This work suggests that a novel approach of targeting pathogen virulence could be achieved at the transcription level in *Yersinia* spp. The *N*-hydroxybenzimidazoles described in this work are effective antivirulence agents in vitro and have the potential to be developed into drug candidates against diseases caused by *Yersinia* spp.

Experimental Section

General. All chemical reactions were carried out under an atmosphere of either argon or nitrogen unless mentioned otherwise. All reagents and solvents were purchased from commercial vendors and used without further purification. The reactions were monitored using an analytical HPLC and/or an LCMS. The analytical HPLC traces were recorded using a Luna C_{18}-phenyl hexyl column (50 mm × 4.6 mm, 5 μm) with either acidic (0.1% v/v CF_3COOH in water as solvent A, 0.1% v/v CF_3COOH in acetonitrile as solvent B) or basic (20 mM triethanolamine in water as solvent A and acetonitrile as solvent B) media with the λ_{det} set at 280 nm. The LCMS (Shimadzu LCMS-2010 EV) spectra were recorded using 0.2% v/v HCOOH in water as solvent A and 0.2% v/v HCOOH in

acetonitrile as solvent B (λ_{det} = 280 nm) with Luna C_{18} Synergi column (50 mm × 4.66 mm, 5 μm) for LC, with the ESI-MS operating in positive mode unless mentioned otherwise. The ^{1}H NMR spectra were recorded in DMSO-d_6 using a Bruker DPX300 NMR spectrometer operating at 300 MHz. The ^{1}H NMR chemical shifts are reported in ppm (δ) relative to the residual protonated solvent peak. The purity of final compounds was assessed based on analytical HPLC, and the results were greater than 95% unless specified otherwise.

Method A: General Synthesis of 4-Aminobenzyl-(2,4-dinitrophenyl)-amine Derivatives (3). To a solution of 4-aminobenzyl amine derivatives (25.5 mL, 225 mmol) and powdered $NaHCO_3$ (94.5 g, 1125 mmol) in anhydrous DMF (300 mL) was added 2,4-dinitrofluoro benzene (18.8 mL, 150 mmol) dropwise at room temperature. After 2 h, the solution was slowly diluted with water (1000 mL) to precipitate the product, which was collected on a fritted funnel rinsing with water until the eluent was colorless. The solid was further dried under high vacuum to afford the product **3** as a bright-orange solid (43 g, 99% yield). This crude material was used for the next step without further purification. ^{1}H NMR (300 MHz, DMSO-d_6) δ 9.18 (t, J = 5.7 Hz, 1H), 8.86 (d, J = 3.0 Hz, 1H), 8.22 (dd, J = 2.7, 9.6 Hz, 1H), 7.13 (d, J = 9.6 Hz, 1H), 7.05 (d, J = 8.4 Hz, 2H), 6.53 (d, J = 8.4 Hz, 2H), 5.05 (s, 2H), 4.54 (d, J = 6.0 Hz, 2H). MS (ESI, positive): calcd for [$C_{13}H_{12}N_4O_4$], 288.26; found, 330.10 [M + H + CH_3CN]$^+$.

General Synthesis of 6-Nitro-2-(4-aminophenyl)-1-hydroxybenzimidazole Derivatives (4). To a solution of *N*-(4-aminobenzyl)-2,4-dinitroaniline derivative **3** (21.6 g, 74.9 mmol) in anhydrous DMF (75 mL) was slowly added NaOMe (30% w/w in MeOH) (67.5 g, 375 mmol) at room temperature under argon atmosphere. After the addition, the solution was warmed to 60 °C for 2 h. After cooling to ambient temperature, the solution was transferred to an Erlenmeyer flask or tall beaker, diluted with water (700 mL), and then acidified with saturated citric acid. The resulting precipitate was collected on a sintered funnel rinsing with water. The crude product was purified by recrystallization in hot EtOH to afford **4** as a brown solid (18.1 g, 90% yield). ^{1}H NMR (300 MHz, DMSO-d_6) δ 12.36 (s, 1H), 8.22 (d, J = 2.4 Hz, 1H), 8.08−8.04 (m, 3H), 7.67 (d, J = 8.7 Hz, 1H), 6.68 (d, J = 8.7 Hz, 2H), 5.91 (br s, 2H). MS (ESI, positive): calcd for [$C_{13}H_{10}N_4O_3$], 270.25; found, 271.05 [M + H]$^+$.

General Synthesis of *N*-Acyl-6-nitro-2-(4-aminophenyl)-1-hydroxybenzimidazole Derivatives (6). To a solution of 6-nitro-2-(4-aminophenyl)-1-hydroxybenzimidazole derivative **4** (1.0 mmol) in anhydrous pyridine (2.0 mL) was added an acid chloride (2.5 mmol) at room temperature. After stirring for 2−3 h, the solution was diluted with 3N NaOH (6.0 mL) and stirred for another hour. The deep-amber solution was transferred to an Erlenmeyer flask or beaker through dilution with water (100 mL) and then acidified with saturated citric acid. The resulting precipitate was collected on a sintered funnel rinsing with water. The crude product **6** was further purified either by preparative HPLC or by recrystallization in hot EtOH.

4-Fluoro-*N*-[4-(1-hydroxy-6-nitro-1*H*-benzoimidazol-2-yl)-benzyl]-benzamide (11). ^{1}H NMR (300 MHz, DMSO-d_6) δ 12.64 (s, 1H), 9.19 (t, J = 5.7 Hz, 1H), 8.39 (d, J = 2.1 Hz, 1H), 8.29 (d, J = 8.4 Hz, 2H), 8.14 (dd, J = 2.4, 9 Hz, 1H), 8.01 (dd, J = 5.7, 8.7 Hz, 2H), 7.85 (d, J = 9 Hz, 1H), 7.55 (d, J = 8.4 Hz, 2H), 7.34 (t, J = 9 Hz, 2H), 4.59 (d, J = 6 Hz, 2H). MS (ESI, positive): calcd for [$C_{21}H_{15}F_1N_4O_4$], 406.38; found, 407.18 [M + H]$^+$.

2-(4-Fluoro-phenyl)-*N*-[4-(1-hydroxy-6-nitro-1*H*-benzoimidazol-2-yl)-phenyl]-acetamide (12). ^{1}H NMR (300 MHz, DMSO-d_6) δ 12.56 (s, 1H), 10.41 (s, 1H), 8.23 (d, J = 2.3 Hz, 1H), 8.20 (d, J = 8.8 Hz, 2H), 8.01 (dd, J = 2.3, 8.9 Hz, 1H), 7.71 (d, J = 8.8 Hz, 2H), 7.70 (d, J = 8.9 Hz, 1H), 7.28 (dd, J = 5.7, 8.6 Hz, 2H), 7.06 (t, J = 8.9 Hz, 2H), 3.60 (s, 2H). MS (ESI, positive): calcd for [$C_{21}H_{15}F_1N_4O_4$], 406.38; found, 407.17 [M + H]$^+$.

3-(4-Fluoro-phenyl)-*N*-[4-(1-hydroxy-6-nitro-1*H*-benzoimidazol-2-yl)-phenyl]-propionamide (13). ^{1}H NMR (300 MHz, DMSO-d_6) δ 12.63 (s, 1H), 10.39 (s, 1H), 8.34 (d, J = 2.2 Hz, 1H), 8.30 (d, J = 8.8 Hz, 2H), 8.12 (dd, J = 2.2, 8.9 Hz, 1H), 7.81 (d, J = 8.9 Hz, 2H, and s, 1H), 7.31 (dd, J = 8.5, 5.8 Hz, 2H), 7.12 (t, J = 8.8 Hz, 2H), 2.94 (t, J = 7.4 Hz, 2H), 2.69 (t, J = 7.8 Hz, 2H). MS (ESI, positive): calcd for [$C_{22}H_{17}F_1N_4O_4$], 420.40; found, 421.09 [M + H]$^+$.

(*E*)-3-(4-Fluoro-phenyl)-*N*-[4-(1-hydroxy-6-nitro-1*H*-benzoimidazol-2-yl)-phenyl]-acrylamide (14). ^{1}H NMR (300 MHz, DMSO-d_6) δ 12.61 (s, 1H), 10.54 (s, 1H), 8.37 (d, J = 2.0 Hz, 1H), 8.35 (d, J = 8.7 Hz, 2H), 8.14 (dd, J = 2.2, 8.9 Hz, 1H), 7.94 (d, J = 8.8 Hz, 2H), 7.83 (d, J = 8.9 Hz, 1H), 7.73 (dd, J = 5.7, 8.6 Hz, 2H), 7.66 (d, J = 15.7 Hz, 1H), 7.31 (t, J = 8.8 Hz, 2H), 6.83 (d, J = 15.7 Hz, 1H). MS (ESI, positive): calcd for [$C_{22}H_{15}F_1N_4O_4$], 418.39; found, 419.08 [M + H]$^+$.

(*E*)-3-(4-Fluoro-phenyl)-*N*-[4-(1-hydroxy-6-nitro-1*H*-benzoimidazol-2-yl)-benzyl]-acrylamide (15). ^{1}H NMR (300 MHz, DMSO-d_6) δ 12.65 (s, 1H), 8.75 (t, J = 5.9 Hz, 1H), 8.39 (d, J = 2.4 Hz, 1H), 8.30 (d, J = 8.4 Hz, 2H), 8.14 (dd, J = 2.4, 9 Hz, 1H), 7.86 (d, J = 9 Hz, 1H), 7.66 (dd, J = 5.7, 8.4 Hz, 2H), 7.53 (d, J = 8.4 Hz, 2H), 7.51 (d, J = 16.2 Hz, 1H), 7.27 (t, J = 9 Hz, 2H), 6.68 (d, J = 15.9 Hz, 1H), 4.52 (d, J = 6 Hz, 2H). MS (ESI, positive): calcd for [$C_{23}H_{17}F_1N_4O_4$], 432.41; found, 433.23 [M + H]$^+$.

(*E*)-*N*-[4-(1-Hydroxy-6-nitro-1*H*-benzoimidazol-2-yl)-phenyl]-3-phenyl-acrylamide (16). ^{1}H NMR (300 MHz, DMSO-d_6) δ 12.65 (s, 1H), 10.51 (s, 1H), 8.32 (d, J = 2.2 Hz, 1H), 8.30 (d, J = 8.8 Hz, 2H), 8.09 (dd, J = 2.3, 8.9 Hz, 1H), 7.90 (d, J = 8.8 Hz, 2H), 7.78 (d, J = 8.9 Hz, 1H), 7.62 (d, J = 8.5 Hz, 2H), 7.61 (d, J = 15.2 Hz, 1H), 7.47−7.37 (m, 3H), 6.85 (d, J = 15.8 Hz, 1H). MS (ESI, positive): calcd for [$C_{22}H_{16}N_4O_4$], 400.40; found, 401.11 [M + H]$^+$.

(*E*)-3-(2,4-Difluoro-phenyl)-*N*-[4-(1-hydroxy-6-nitro-1*H*-benzoimidazol-2-yl)-phenyl]-acrylamide (17). ^{1}H NMR (300 MHz, DMSO-d_6) δ 12.62 (br s, 1H), 10.62 (s, 1H), 8.34 (d, J = 2.2 Hz, 1H), 8.33 (d, J = 8.7 Hz, 2H), 8.11 (dd, J = 2.4, 9 Hz, 1H), 7.93 (d, J = 9 Hz, 2H), 7.81 (d, J = 9 Hz, 1H), 7.78 (t, J = 8.7 Hz, 1H), 7.63 (d, J = 15.9 Hz, 1H), 7.39 (dt, J = 2.7, 9.6 Hz, 1H), 7.21 (dt, J = 2.1, 8.4 Hz, 1H), 6.94 (d, J = 15.9 Hz, 1H). MS (ESI, positive): calcd for [$C_{22}H_{14}F_2N_4O_4$], 436.38; found, 437.08 [M + H]$^+$.

(*E*)-3-(3,4-Difluoro-phenyl)-*N*-[4-(1-hydroxy-6-nitro-1*H*-benzoimidazol-2-yl)-phenyl]-acrylamide (18). ^{1}H NMR (300 MHz, DMSO-d_6) δ 12.64 (br, 1H), 10.62 (s, 1H), 8.37 (d, J = 2.4 Hz, 1H), 8.35 (d, J = 8.7 Hz, 2H), 8.14 (dd, J = 2.4, 9 Hz, 1H), 7.94 (d, J = 9.0 Hz, 2H), 7.84 (d, J = 9.0 Hz, 1H), 7.77 (m, 1H), 7.63 (d, J = 15.9 Hz, 1H), 7.57−7.53 (m, 2H), 6.87 (d, J = 15.6 Hz, 1H). MS (ESI, positive): calcd for [$C_{22}H_{14}F_2N_4O_4$], 436.38; found, 437.15 [M + H]$^+$.

(*E*)-*N*-[4-(1-Hydroxy-6-nitro-1*H*-benzoimidazol-2-yl)-phenyl]-3-*p*-tolyl-acrylamide (20). ^{1}H NMR (300 MHz, DMSO-d_6) δ 12.63 (s, 1H), 10.52 (s, 1H), 8.37 (d, J = 2.4 Hz, 1H), 8.35 (d, J = 9 Hz, 2H), 8.13 (dd, J = 2.1, 8.7 Hz, 1H), 7.94 (d, J = 9 Hz, 2H), 7.83 (d, J = 9 Hz, 1H), 7.61 (d, J = 15.9 Hz, 1H), 7.55 (d, J = 8.1 Hz, 2H), 7.28 (d, J = 7.8 Hz, 2H), 6.83 (d, J = 15.6 Hz, 1H), 2.35 (s, 3H). MS (ESI, positive): calcd for [$C_{23}H_{18}N_4O_4$], 414.42; found, 415.15 [M + H]$^+$.

(*E*)-*N*-[4-(1-Hydroxy-6-nitro-1*H*-benzoimidazol-2-yl)-phenyl]-3-(2-methoxy-phenyl)-acrylamide (21). ^{1}H NMR (300 MHz, DMSO-d_6) δ 12.58 (s, 1H), 10.46 (s, 1H), 8.30 (d, J = 2.0 Hz, 1H), 8.29 (d, J = 8.6 Hz, 2H), 8.08 (dd, J = 2.2, 8.9 Hz, 1H), 7.89 (d, J = 8.8 Hz, 2H), 7.81 (d, J = 14.4 Hz, 1H), 7.77 (d, J = 8.8 Hz, 1H), 7.56 (d, J = 7.6 Hz, 1H), 7.37 (t, J = 8.3 Hz, 1H), 7.07 (d, J = 8.3 Hz, 1H), 6.99 (t, J = 7.5 Hz, 1H), 6.88 (d, J = 15.8 Hz, 1H), 3.86 (s, 3H). MS (ESI, positive): calcd for [$C_{23}H_{18}N_4O_5$], 430.42; found, 431.14 [M + H]$^+$.

(*E*)-*N*-[4-(1-Hydroxy-6-nitro-1*H*-benzoimidazol-2-yl)-phenyl]-3-(4-methoxy-phenyl)-acrylamide (22). ^{1}H NMR (300 MHz, DMSO-d_6) δ 12.57 (s, 1H), 10.40 (s, 1H), 8.31 (d, J = 2.3 Hz, 1H), 8.28 (d, J = 9.0 Hz, 2H), 8.08 (dd, J = 2.3, 8.9 Hz, 1H), 7.88 (d, J = 8.9 Hz, 2H), 7.77 (d, J = 8.9 Hz, 1H), 7.56 (d, J = 9.0 Hz, 2H), 7.55 (d, J = 14.6 Hz, 1H), 6.97 (d, J = 8.7 Hz, 2H), 6.68 (d,

J = 15.7 Hz, 1H), 3.76 (s, 3H). MS (ESI, positive): calcd for $[C_{23}H_{18}N_4O_5]$, 430.42; found, 431.14 $[M + H]^+$.

(*E*)-3-(2,4-Dimethoxy-phenyl)-*N*-[4-(1-hydroxy-6-nitro-1*H*-benzoimidazol-2-yl)-phenyl]-acrylamide (24). ^{1}H NMR (300 MHz, DMSO-d_6) δ 12.62 (br s, 1H), 10.43 (s, 1H), 8.36 (d, J = 2.4 Hz, 1H), 8.33 (d, J = 9 Hz, 2H), 8.13 (dd, J = 2.1, 9 Hz, 1H), 7.94 (d, J = 8.7 Hz, 2H), 7.83 (d, J = 9 Hz, 1H), 7.78 (d, J = 16.8 Hz, 1H), 7.54 (d, J = 8.4 Hz, 1H), 6.81 (d, J = 15.6 Hz, 1H), 6.65−6.62 (m, 2H), 3.91 (s, 3H), 3.83 (s, 3H). MS (ESI, positive): calcd for $[C_{24}H_{20}N_4O_6]$, 460.45; found, 461.25 $[M + H]^+$.

(*E*)-*N*-[4-(1-Hydroxy-6-nitro-1*H*-benzoimidazol-2-yl)-phenyl]-3-(4-isopropyl-phenyl)-acrylamide (25). ^{1}H NMR (300 MHz, DMSO-d_6) δ 12.64 (br s, 1H), 10.54 (s, 1H), 8.36 (br s, 1H), 8.35 (d, J = 8.7 Hz, 2H), 8.12 (dd, J = 2.3, 8.9 Hz, 1H), 7.93 (d, J = 8.8 Hz, 2H), 7.81 (d, J = 8.9 Hz, 1H), 7.62 (d, J = 15.5 Hz, 1H), 7.58 (d, J = 8.0 Hz, 2H), 7.34 (d, J = 8.1 Hz, 2H), 6.84 (d, J = 15.7 Hz, 1H), 2.93 (m, J = 6.9 Hz, 1H), 1.23 (dd, J = 6.9 Hz, 6H). MS (ESI, positive): calcd for $[C_{25}H_{22}N_4O_4]$, 442.48; found, 443.26 $[M + H]^+$.

(*E*)-3-(4-Dimethylamino-phenyl)-*N*-[4-(1-hydroxy-6-nitro-1*H*-benzoimidazol-2-yl)-phenyl]-acrylamide (26). ^{1}H NMR (300 MHz, DMSO-d_6) δ 12.61 (s, 1H), 10.28 (s, 1H), 8.29 (d, J = 2.0 Hz, 1H), 8.27 (d, J = 8.7 Hz, 2H), 8.07 (dd, J = 2.3, 8.9 Hz, 1H), 7.86 (d, J = 8.9 Hz, 2H), 7.76 (d, J = 8.9 Hz, 1H), 7.48 (d, J = 15.5 Hz, 1H), 7.42 (d, J = 8.9, 2H), 6.71 (d, J = 8.9, 2H), 6.55 (d, J = 15.5 Hz, 1H), 2.93 (s, 6H). MS (ESI, positive): calcd for $[C_{24}H_{21}N_5O_4]$, 443.47; found, 444.14 $[M + H]^+$.

(*E*)-3-(4-Fluoro-phenyl)-*N*-[5-(1-hydroxy-6-nitro-1*H*-benzoimidazol-2-yl)-pyridin-2-yl]-acrylamide (30). ^{1}H NMR (300 MHz, DMSO-d_6) δ 12.81 (s, 1H), 11.10 (s, 1H), 9.27 (d, J = 1.8 Hz, 1H), 8.71 (dd, J = 2.4, 8.7 Hz, 1H), 8.47 (d, J = 9.0 Hz, 1H), 8.41 (d, J = 1.8 Hz, 1H), 8.15 (dd, J = 2.4, 8.7 Hz, 1H), 7.87 (d, J = 9.0 Hz, 1H), 7.73−7.68 (m, 3H), 7.32 (t, J = 8.7 Hz, 2H), 7.03 (d, J = 15.6 Hz, 1H). MS (ESI, positive): calcd for $[C_{21}H_{14}F_1N_5O_4]$, 419.38; found, 420.10 $[M + H]^+$.

(*E*)-3-(4-Fluoro-phenyl)-*N*-[6-(1-hydroxy-6-nitro-1*H*-benzoimidazol-2-yl)-pyridin-3-yl]-acrylamide (31). ^{1}H NMR (300 MHz, DMSO-d_6) δ 12.83 (br s, 1H), 10.79 (s, 1H), 9.09 (br s, 1H), 8.42−8.33 (m, 3H), 8.16 (dd, J = 1.8, 8.7 Hz, 1H), 7.88 (d, J = 8.7 Hz, 1H), 7.75 (dd, J = 5.4, 8.4 Hz, 2H), 7.70 (d, J = 15.6 Hz, 1H), 7.32 (t, J = 8.7 Hz, 2H), 6.82 (d, J = 15.6 Hz, 1H). MS (ESI, positive): calcd for $[C_{21}H_{14}F_1N_5O_4]$, 419.38; found, 420.15 $[M + H]^+$.

(*E*)-*N*-[3-Fluoro-4-(1-hydroxy-6-nitro-1*H*-benzoimidazol-2-yl)-phenyl]-3-(4-fluoro-phenyl)-acrylamide (33). ^{1}H NMR (300 MHz, DMSO-d_6) δ 12.47 (s, 1H), 10.72 (s, 1H), 8.39 (d, J = 2.1 Hz, 1H), 8.17 (dd, J = 2.2, 8.9 Hz, 1H), 7.99−7.84 (m, 1H), 7.88 (d, J = 8.8 Hz, 2H), 7.76−7.56 (m, 4H), 7.31 (t, J = 8.8 Hz, 2H), 6.80 (d, J = 15.7 Hz, 1H). MS (ESI, positive): calcd for $[C_{22}H_{14}F_2N_4O_4]$, 436.38; found, 437.15 $[M + H]^+$.

(*E*)-3-(4-Fluoro-phenyl)-*N*-[4-(1-hydroxy-6-nitro-1*H*-benzoimidazol-2-yl)-2-methyl-phenyl]-acrylamide (34). ^{1}H NMR (300 MHz, DMSO-d_6) δ 12.68 (s, 1H), 9.58 (s, 1H), 8.36 (d, J = 2.2 Hz, 1H), 8.22−8.18 (m, 2H), 8.13 (dd, J = 2.3, 8.9 Hz, 1H), 8.03 (dd, J = 8.4 Hz, 1H), 7.83 (d, J = 8.9 Hz, 1H), 7.73 (dd, J = 5.6, 8.7 Hz, 2H), 7.64 (d, J = 15.7 Hz, 1H), 7.31 (t, J = 8.8 Hz, 2H), 7.05 (d, J = 15.7 Hz, 1H), 2.41 (s, 3H). MS (ESI, positive): calcd for $[C_{23}H_{17}F_1N_4O_4]$, 432.41; found, 433.10 $[M + H]^+$.

(*E*)-3-(4-Fluoro-phenyl)-*N*-[4-(1-hydroxy-5-methyl-6-nitro-1*H*-benzoimidazol-2-yl)-phenyl]-acrylamide (36). ^{1}H NMR (300 MHz, DMSO-d_6) δ 12.59 (s, 1H), 10.52 (s, 1H), 8.31 (d, J = 8.7 Hz, 2H), 8.17 (s, 1H), 7.91 (d, J = 8.8 Hz, 2H), 7.75−7.62 (m, 4H), 7.31 (t, J = 8.8 Hz, 2H), 6.82 (d, J = 15.7 Hz, 1H), 2.63 (s, 3H). MS (ESI, positive): calcd for $[C_{23}H_{17}F_1N_4O_4]$, 432.41; found, 433.10 $[M + H]^+$.

(*E*)-*N*-[4-(6-Cyano-1-hydroxy-1*H*-benzoimidazol-2-yl)-phenyl]-3-(4-fluoro-phenyl)-acrylamide (45). ^{1}H NMR (300 MHz, DMSO-d_6) δ 12.44 (br s, 1H), 10.53 (s, 1H), 8.31 (d, J = 8.8 Hz, 2H), 8.08 (br s, 1H), 7.92 (d, J = 8.8 Hz, 2H), 7.81 (d, J = 8.4 Hz, 1H), 7.75−7.60 (m, 4H), 7.31 (t, J = 8.8 Hz, 2H), 6.83 (d, J = 15.7 Hz, 1H). MS (ESI, positive): calcd for $[C_{23}H_{15}F_1N_4O_2]$, 398.40; found, 399.17 $[M + H]^+$.

(*E*)-3-(4-Fluoro-phenyl)-*N*-[4-(1-hydroxy-6-pyrazol-1-yl-1*H*-benzoimidazol-2-yl)-phenyl]-acrylamide (50). To a solution of 4-aminobenzyl amine (35.4 mL, 313 mmol) and powdered $NaHCO_3$ (158 g, 1875 mmol) in anhydrous DMF (500 mL) at room temperature was added a solution of 4-bromo-1-fluoro-2-nitrobenzene (31.4 mL, 250 mmol) in anhydrous DMF (50 mL) dropwise via addition funnel over 1 h period. After another 4 h, the solution was diluted with anhydrous absolute EtOH (1000 mL) and powdered KO^{t}Bu (140 g, 1250 mmol) was added in portions. This solution was subsequently heated to 60 °C for 6 h. After cooling to room temperature, the solution was poured into a stirring solution of water (4 L) and then adjusted to pH 6 with 1 M HCl. The slowly stirring suspension was cooled with an ice bath to facilitate solidification. The suspended product was collected on a fine fritted funnel and rinsed with water until the eluent was colorless. The orange solid was further dried under high vacuum. A 20 mL Biotage microwave vial was charged with 6-bromo-2-(4-aminophenyl)-1-hydroxybenzimidazole (1.5 g, 5.0 mmol), *N*,*N*′-dimethylethylenediamine (1.1 mL, 10.0 mmol), CuI (0.9 g, 5.0 mmol), pyrazole (1.4 g, 20.0 mmol), KO^{t}Bu (2.3 g, 20.0 mmol), and anhydrous DMSO (20 mL). The secured vial was placed into a Biotage microwave reactor with a temperature setting of 195 °C for 45 min. After cooling, the vial was opened and poured into a rapidly stirring water solution. The resulting suspension was filtered through a plug of celite, rinsing with 0.5 M NaOH. The water solution was loaded onto a prepared DVB column. After loading, the product was eluted with acetonitrile. The acetonitrile was removed under reduced pressure. The resulting water solution was cooled to 0 °C with an ice bath, and then the solution pH was adjusted to 6 with 1 M HCl to precipitate the product. The resulting solid was collected and rinsed with cold water. After further drying under vacuum, the product **50** was obtained as a light-brown solid. ^{1}H NMR (300 MHz, DMSO-d_6) δ 12.22 (br, 1H), 10.50 (s, 1H), 8.59 (s, 1H), 8.26 (d, J = 8.1 Hz, 2H), 7.93 (s, 1H), 7.90 (d, J = 8.4 Hz, 2H), 7.75−7.66 (m, 5H), 7.63 (d, J = 15.9 Hz, 1H), 7.29 (t, J = 8.4 Hz, 2H), 6.82 (d, J = 15.6 Hz, 1H), 6.55 (s, 1H). MS (ESI, positive): calcd for $[C_{25}H_{18}F_1N_5O_2]$, 439.45; found, 440.20 $[M + H]^+$.

Method B: General Synthesis of 4-Phenylamidobenzylamine Derivatives (7). To a solution of 4-cyanoaniline derivative (225 mmol) in pyridine or *N*-methylpyrrolidone (180 mL) was added a cinnamoyl chloride (225 mmol) over a period of 3−5 min with vigorous stirring. After stirring the reaction mixture for 5 h (until HPLC monitoring of the reaction indicated a complete consumption of the starting materials), it was poured into 1400 mL of water at room temperature and the resulting suspension was stirred for 1 h. The precipitate was filtered, washed with 4 × 500 mL portions of water and dried. A second crop of solid was obtained from the filtrate and washings. The solids were combined and used for the next step without further purification. In a pressure reactor, 4-phenylamido benzonitrile intermediate (98 mmol) was dissolved in anhydrous THF (940 mL) and the solution was purged with argon for 2−3 min, followed by the addition of 11 mL of the uniformly suspended catalyst (Raney nickel 2400, suspension in water). After addition of a small amount of MeOH to the suspension, the reactor was pressurized at 55 psi of H_2 while stirring vigorously. LCMS monitoring of the reaction indicated a complete conversion of the starting material to the corresponding amine within 2.5 h. The reaction mixture was filtered over a bed of diatomaceous earth (e.g., celite), and washed with 3 × 100 mL portions of anhydrous THF. The combined filtrates were evaporated to dryness and further dried under high vacuum to afford **7** as a white colored solid. The crude product was used for the next step without further characterization.

(*E*)-*N*-{4-[(5-Fluoro-2,4-dinitro-phenylamino)-methyl]-phenyl}-3-phenyl-acrylamide (8). To a solution of 1,5-difluoro-2,4-dinitrobenzene (0.8 g, 3.9 mmol) in 30 mL of DMF was added sodium

bicarbonate (3.3 g, 39 mmol) and the intermediate **7** (1.5 g, 3.9 mmol). The reaction mixture was stirred at room temperature for 3 h and then poured into ice−water to give a precipitate. The precipitate was filtered, washed with water, and dried under vacuum to give the desired product **8** (1.6 g, 90% yield). This material was used for the next step without further purification. ^{1}H NMR (300 MHz, DMSO-d_6) δ 10.21 (s, 1H), 9.40 (t, J = 6 Hz, 1H), 8.89 (d, J = 8.1 Hz, 1H), 7.71−7.66 (m, 4H), 7.58 (d, J = 15.6 Hz, 1H), 7.37 (d, J = 8.4 Hz, 2H), 7.28 (t, J = 8.7 Hz, 2H), 7.00 (d, J = 15 Hz, 1H), 6.76 (d, J = 15.6 Hz, 1H), 4.70 (d, J = 6 Hz, 2H). MS (ESI, positive): calcd for [$C_{22}H_{16}F_2N_4O_5$], 454.39; found, 455.15 [M + H]$^+$.

(*E*)-*N*-[4-(5-Ethoxy-1-hydroxy-6-nitro-1*H*-benzoimidazol-2-yl)-phenyl]-3-(4-fluoro-phenyl)-acrylamide (37). To a solution of **8** (0.2 g, 0.4 mmol) in EtOH (10 mL) and DMF (10 mL), was added NaH (60% w/w in mineral oil) (88 mg, 2.2 mmol). The reaction mixture was heated at 60 °C for 3 h. After cooling to room temperature, it was poured into ice−water and acidified with aqueous citric acid. The resulting precipitates were collected, washed with water, and purified by preparative HPLC. Fractions showing >95% purity by analytical HPLC were combined, and the volatiles were evaporated under vacuum. The resulting solid was collected and washed with water. After drying under vacuum, the product **37** was obtained as a yellow solid. ^{1}H NMR (300 MHz, DMSO-d_6) δ 12.41 (s, 1H), 10.51 (s, 1H), 8.29 (d, J = 8.7 Hz, 2H), 8.05 (s, 1H), 7.91 (d, J = 8.8 Hz, 2H), 7.72 (dd, J = 5.7, 8.5 Hz, 2H), 7.65 (d, J = 15.7 Hz, 1H), 7.50 (s, 1H), 7.30 (t, J = 8.8 Hz, 2H), 6.82 (d, J = 15.7 Hz, 1H), 4.22 (qr, J = 6.9 Hz, 2H), 1.37 (t, J = 6.9 Hz, 3H). MS (ESI, positive): calcd for [$C_{24}H_{19}F_1N_4O_5$], 462.44; found, 463.15 [M + H]$^+$.

(*E*)-*N*-[4-(5-Dimethylamino-1-hydroxy-6-nitro-1*H*-benzoimidazol-2-yl)-phenyl]-3-(4-fluoro-phenyl)-acrylamide (39). To a solution of **8** (0.9 g, 2 mmol) in DMF (50 mL) was added $NaHCO_3$ (1.7 g, 20 mmol), followed by 4 mL of 2.0 M dimethylamine solution in THF (8 mmol). After stirring at RT for 3 h, the reaction mixture was poured into water (500 mL). After filtration, the collected solid was washed with water and dried under vacuum, resulting in (*E*)-*N*-{4-[(5-dimethylamino-2,4-dinitro-phenylamino)-methyl]-phenyl}-3-(4-fluoro-phenyl)-acrylamide intermediate as a yellow solid (0.8 g, 84% yield). This crude material was used for the next step. To a solution of the aforementioned intermediate (0.8 g, 1.7 mmol) in DMF (30 mL) was added NaOMe (30% w/w in MeOH) (1.5 g, 8.4 mmol). The reaction mixture was heated at 60 °C for 3 h. After cooling to room temperature, it was poured into ice−water and acidified with aqueous citric acid. The resulting precipitation was collected, washed with water, and purified by preparative HPLC. Fractions showing greater than 95% purity by analytical HPLC were combined and concentrated. The resulting solid was collected and washed with water. After drying under vacuum, the product **39** was obtained as a yellow solid. ^{1}H NMR (300 MHz, DMSO-d_6) δ 12.32 (s, 1H), 10.52 (s, 1H), 8.28 (d, J = 8.8 Hz, 2H), 7.98 (s, 1H), 7.91 (d, J = 8.9 Hz, 2H), 7.74−7.70 (m, 2H), 7.65 (d, J = 15.7 Hz, 1H), 7.49 (s, 1H), 7.31 (t, J = 8.8 Hz, 2H), 6.82 (d, J = 15.7 Hz, 1H), 2.75 (s, 6H). MS (ESI, positive): calcd for [$C_{24}H_{20}F_1N_5O_4$], 461.46; found, 462.15 [M + H]$^+$.

Cell-Free LcrF−DNA Binding Assay. A biotinylated double-stranded DNA molecule (2 nM), containing the LcrF binding sequences, was incubated with 6His-LcrF (20 nM) in a streptavidin coated 96-well microtiter plate (Thermo Lab Systems, Waltham, MA) in the presence of varying concentrations of an inhibitor and in assay buffer (20 mM Hepes, 10 mM ammonium sulfate, 30 mM potassium chloride, 1 mM EDTA, 0.2% polysorbate 20, and 0.5% nonfat dry milk). Unbound DNA and the protein were removed by washing, and a primary monoclonal anti-6His antibody was then added. Bound DNA−protein complexes were detected by a secondary horseradish peroxidase (HRP)-conjugated antibody acting on a chemiluminescence substrate (Cell Signaling Technology, Beverly, MA). Luminescence was measured on a Victor V plate reader (PerkinElmer Life Sciences, Wellesley, MA). Luminescence data were converted to % LcrF binding inhibition by comparison to control wells. The % LcrF binding inhibition data for each test compound titration were plotted in Microsoft Excel, and XLfit (IDBS) was used to fit the dose−response curve and reported as IC_{50} (test compound concentration that inhibited LcrF binding by 50%). ExsA−DNA binding and SlyA−DNA binding assays were carried out by following a similar procedure. Data represent the average values from two independent experiments for most compounds. IC_{50} data for compounds **10**, **14**, **17**, **24**, **26**, **45**, and **52** are the median values from at least three independent experiments (see Supporting Information).

Whole Cell Assay: Inhibition of *Yersinia* Cytotoxicity in J774A.1 Macrophages. The cytotoxicity assay was based on the protocol by Monack et al. described previously.[24] J774A.1 macrophages were plated at 2×10^4 cells per well in 96-well plates on the day prior to infection. Overnight cultures of wild-type (YPIIIpIB1)[23] or the *lcrF* deletion mutant (YPIIIpIB1Δ*lcrF*)[25] strains of *Y. pseudotuberculosis* were diluted into 2-YT broth supplemented with 20 mM magnesium chloride and 20 mM sodium oxalate. Cultures were grown for 90 min at 26 °C and then shifted to 37 °C for 90 min to induce LcrF expression. Bacteria were added to cells in DMEM (Invitrogen, Carlsbad, CA) and incubated at 37 °C with 5% CO_2 for 2 h. The multiplicity of infection was 5−10 bacteria per J774A.1 cell. Gentamicin was added at 50 μg/mL to kill extracellular bacteria, and incubations continued overnight (~18 h). Supernatants containing released LDH (lactate dehydrogenase), an indication of cell death, were assayed colorimetrically using the Cytox 96 kit from Promega (Madison, WI). Test compounds at 50 μg/mL were added to the *Yersinia* culture media and to the J774A.1 cell wells during infections. Control cultures and wells received an equal volume of vehicle (DMSO with 0.4% ethanolamine). Results are expressed as % wild-type cytotoxicity (the amount of LDH released in wells infected with wild-type *Y. pseudotuberculosis* in the presence of vehicle alone).

In Vitro Antimicrobial Susceptibility Test. The minimum inhibitory concentration (MIC) of test compounds were determined using Clinical Laboratory Standards Institute (CLSI) methodology.[41] On each day of testing, serial dilutions of compounds were prepared in microdilution plates using a Tecan robotic workstation. Mueller Hinton broth cultures of strains were grown or adjusted to match the turbidity of a 0.5 McFarland standard. Dilutions of 1:100 were made in an appropriate broth to achieve a final inoculum of 5×10^5 cells/mL. Plates were incubated at 35 °C in ambient air for 18−24 h, read spectrophotometrically, and checked manually for evidence of bacterial growth. The lowest dilution of a compound that inhibited bacterial growth was recorded as the MIC.

In Vitro DNA Binding Assay. To assess nonspecific DNA binding, the effects of compounds on the migration of a supercoiled plasmid DNA during agarose gel electrophoresis were tested. Compounds were diluted in DMSO with 0.4% ethanolamine to a concentration of 1 mg/mL. In a clear 96-well plate, 2 μL of 1 mg/mL compound solution was added to 18 μL of assay buffer (20 mM Hepes, pH 7.6, 10 mM ammonium sulfate, 30 mM potassium chloride, 1 mM EDTA, 0.2% polysorbate 20) containing 100 ng of pET-15b supercoiled plasmid DNA. The final concentration of test compounds was therefore 100 μg/mL. The plate was incubated at room temperature for 30 min. Then 10 microliters of compound and DNA solutions were loaded onto a 0.8% agarose gel and subjected to electrophoresis. The gel was then stained with ethidium bromide and photographed. Control tests with drug vehicle (DMSO with 0.4% ethanolamine) did not affect DNA migration through the gel. In contrast, tests with 100 μg/mL of positive control Hoechst 33342 dye, a known DNA intercalator, resulted in a faint smear on the gel rather than the discrete bands seen when unperturbed DNA is electrophoresed.

Acknowledgment. This work was supported in part by a grant from the National Institutes of Allergy and Infectious Disease (NIAID) (grant R43 AI058627-01 A1). We thank Joan C. Mecsas and Warangkhana Songsungthong at Tufts University School of Medicine for providing *Y. pseudotuberculosis* strains. We also appreciate the helpful suggestions of Michael P. Draper and Haregewein Assefa in preparing the manuscript.

Supporting Information Available: Compound yields, purities, HPLC conditions for purity determination, additional spectral data for final compounds, and individual IC_{50} values. This material is available free of charge via the Internet at http://pubs.acs.org.

References

(1) Perry, R. D.; Fetherston, J. D. *Yersinia pestis*—etiologic agent of plague. *Clin. Microbiol. Rev.* **1997**, *10*, 35–66.
(2) Hawley, R. J.; Eitzen, E. M. Biological weapons—a primer for microbiologists. *Annu. Rev. Microbiol.* **2001**, *55*, 235–253.
(3) Welch, T. J.; Fricke, W. F.; McDermott, P. F.; White, D. G.; Rosso, M.-L.; Rasko, D. A.; Mammal, M. K.; Eppinger, M.; Rosovitz, M. J.; Wagner, D.; Rahalison, L.; LeClerc, J. E.; Hinshaw, J. M.; Lindler, L. E.; Cebula, T. A.; Carniel, E.; Ravel, J. Multiple antimicrobial resistance in plague: an emerging public health risk. *PLoS ONE* **2007**, *2*, e309.
(4) Levy, S. B. Antibiotic resistance—the problem intensifies. *Adv. Drug. Delivery Rev.* **2005**, *57*, 1446–1450.
(5) Talbot, G. H.; Bradley, J.; Edwards, J. E., Jr.; Gilbert, D.; Scheld, M.; Bartlett, J. G. Bad bugs need drugs: an update on the development pipeline from the Antimicrobial Availability Task Force of the Infectious Disease Society of America. *Clin. Infect. Dis.* **2006**, *42*, 657–668.
(6) Projan, S. J.; Bradford, P. A. Late stage antibacterial drugs in the clinical pipeline. *Curr. Opin. Microbiol.* **2007**, *10*, 441–446.
(7) Clatworthy, A. E.; Pierson, E.; Hung, D. T. Targeting virulence: a new paradigm for antimicrobial therapy. *Nat. Chem. Biol.* **2007**, *3*, 541–548.
(8) Alekshun, M. N.; Levy, S. B. Targeting virulence to prevent infection: to kill or not to kill? *Drug Discovery Today: Ther. Strategies* **2004**, *1*, 483–489.
(9) Alksne, L. E.; Projan, S. J. Bacterial virulence as a target for antimicrobial chemotherapy. *Curr. Opin. Biotechnol.* **2000**, *11*, 625–636.
(10) Bowser, T. E.; Bartlett, V. J.; Grier, M. C.; Verma, A. K.; Warchol, T.; Levy, S. B.; Alekshun, M. N. Novel anti-infection agents: small-molecule inhibitors of bacterial transcription factors. *Bioorg. Med. Chem. Lett.* **2007**, *17*, 5652–5655.
(11) Multiple adaptational response (MAR) proteins are defined as a subgroup of the AraC family transcription factors that control the virulence of bacteria. A subset of MAR proteins may also control antibiotic resistance (see ref 12).
(12) Seoane, A. S.; Levy, S. B. Characterization of MarR, the repressor of the multiple antibiotic resistance (*mar*) operon in *Escherichia coli*. *J. Bacteriol.* **1995**, *177*, 3414–3419.
(13) Casaz, P.; Garrity-Ryan, L. K.; McKenney, D.; Jackson, C.; Levy, S. B.; Tanaka, S. K.; Alekshun, M. N. MarA, SoxS and Rob function as virulence factors in an *Escherichia coli* murine model of ascending pyelonephritis. *Microbiology* **2006**, *152*, 3643–3650.
(14) Egan, S. M. Growing repertoire of AraC/XylS activators. *J. Bacteriol.* **2002**, *184*, 5529–5532.
(15) Gallegos, M.; Schleif, R.; Bairoch, A.; Hofmann, K.; Ramos, J. AraC/XylS family of transcriptional regulators. *Microbiol. Mol. Biol. Rev.* **1997**, *61*, 393–410.
(16) Flashner, Y.; Mamroud, E.; Tidhar, A.; Ber, R.; Aftalion, M.; Gur, D.; Lazar, S.; Zvi, A.; Bino, T.; Ariel, N.; Velan, B.; Shafferman, A.; Cohen, S. Generation of *Yersinia pestis* attenuated strains by signature-tagged mutagenesis in search of novel vaccine candidates. *Infect. Immun.* **2004**, *72*, 908–915.
(17) Champion, G. A.; Neely, M. N.; Brennan, M. A.; DiRita, V. J. A branch in the ToxR regulatory cascade of *Vibrio cholerae* revealed by characterization of *toxT* mutant strains. *Mol. Microbiol.* **1997**, *23*, 323–331.
(18) Bieber, D.; Ramer, S. W.; Wu, C. Y.; Murray, W. J.; Tobe, T.; Fernandez, R.; Schoolnik, G. K. Type IV pili, transient bacterial aggregates, and virulence of enteropathogenic *Escherichia coli*. *Science* **1998**, *280*, 2114–2118.
(19) Hoe, N. P.; Minion, F. C.; Goguen, J. D. Temperature sensing in *Yersinia pestis*: regulation of *yopE* transcription by *lcrF*. *J. Bacteriol.* **1992**, *174*, 4275–4286.
(20) Mota, L. J.; Cornelis, G. R. The bacterial injection kit: type III secretion systems. *Ann. Med.* **2005**, *37*, 234–249.
(21) Cornelis, G. R.; Wolf-Watz, H. The *Yersinia* Yop virulon: a bacterial system for subverting eukaryotic cells. *Mol. Microbiol.* **1997**, *23*, 861–867.
(22) Logsdon, L. K.; Mecsas, J. Requirement of the *Yersinia pseudotuberculosis* effectors YopH and YopE in colonization and persistence in intestinal and lymph tissues. *Infect. Immun.* **2003**, *71*, 4595–4607.
(23) Mecsas, J.; Bilis, I.; Falkow, S. Identification of attenuated *Yersinia pseudotuberculosis* strains and characterization of an orogastric infection in BALB/c mice on day 5 postinfection by signature-tagged mutagenesis. *Infect. Immun.* **2001**, *69*, 2779–2787.
(24) Monack, D. M.; Mecsas, J.; Bouley, D.; Falkow, S. *Yersinia*-induced apoptosis in vivo aids in the establishment of a systemic infection of mice. *J. Exp. Med.* **1998**, *188*, 2127–2137.
(25) Garrity-Ryan, L. K.; Kim, O. K.; Balada-Llasat, J.-M.; Bartlett, V. J.; Verma, A. K.; Fisher, M. L.; Castillo, C.; Songsungthong, W.; Tanaka, S. K.; Levy, S. B.; Mecsas, J.; Alekshun, M. N. Unpublished results: in our own experiment, deletion of the *lcrF* gene exhibited a similar effect of attenuating virulence of *Y. pseudotuberculosis*.
(26) Nordfelth, R.; Kauppi, A. M.; Norberg, H. A.; Wolf-Watz, H.; Elofsson, M. Small-molecule inhibitors specifically targeting type III secretion. *Infect. Immun.* **2005**, *73*, 3104–3114.
(27) Kauppi, A. M.; Nordfelth, R.; Uvell, H.; Wolf-Watz, H.; Elofsson, M. Targeting bacterial virulence: inhibitors of type III secretion in *Yersinia*. *Chem. Biol.* **2003**, *10*, 241–249.
(28) Pan, N. J.; Brady, M. J.; Leong, J. M.; Goguen, J. D. Targeting type III secretion in *Yersinia pestis*. *Antimicrob. Agents Chemother.* **2009**, *53*, 385–392.
(29) Of all peer-reviewed articles searched through SciFinder and Google Scholar, Elofsson et al. suggested that select small molecule inhibitors of T3SS in *Yersinia* might directly interact with LcrF. However, based on the experimental data, they either ruled out the possibility, or concluded it was unknown (see refs 26 and 27).
(30) Kwon, H. J.; Bennik, M. H. J.; Demple, B.; Ellenberger, T. Crystal structure of the *Escherichia coli* Rob transcription factor in complex with DNA. *Nat. Struct. Biol.* **2000**, *7*, 424–430.
(31) Rhee, S.; Martin, R. G.; Rosner, J. L.; Davies, D. R. A novel DNA-binding motif in MarA: The first structure for an AraC family transcriptional activator. *Proc. Natl. Acad. Sci. U.S.A.* **1998**, *95*, 10413–10418.
(32) Proteins were aligned using the BLASTp program on the National Center for Biotechnology Information (NCBI) Web site: http://www.ncbi.nlm.nih.gov
(33) Gardiner, J. M.; Procter, J. Synthesis of *N*-alkoxybenzimidazoles with differentiated C2 and O-substituents. *Tetrahedron Lett.* **2001**, *42*, 5109–5111.
(34) DeStevens, G.; Brown, A. B.; Rose, D.; Chernov, H. I.; Plummer, A. J. Derivatives of 1-hydroxybenzimidazoles and 1-hydroxyindoles and their central depressant effects. *J. Med. Chem.* **1967**, *10*, 211–214.
(35) Wermuth, C. G. Molecular variations based on isosteric replacements. In *The Practice of Medicinal Chemistry*; Wermuth, C. G. Ed.; Academic Press Limited: London, 1996; pp 203–247.
(36) Ohmori, J.; Sakamoto, S.; Kubota, H.; Shimizu-Sasamata, M.; Okada, M.; Kawasaki, S.; Hidaka, K.; Togami, J.; Furuya, T.; Murase, K. 6-(1*H*-imidazol-l-y1)-7-nitro-2,3(1*H*,4*H*)-quinoxalinedione hydrochloride (YM90K) and related compounds: Structure—activity relationships for the AMPA-type non-NMDA receptor. *J. Med. Chem.* **1994**, *37*, 467–475.
(37) In the whole cell cytotoxicity assay, *Y. pseudotuberculosis* was used instead of *Y. pestis* in order to address biosafety concerns associated with *Y. pestis* (category A pathogen). The chromosomes of *Y. pestis* and *Y. pseudotuberculosis* are highly similar, and these two pathogens possess a common set of virulence factors including LcrF (see ref 38).
(38) Achtman, M.; Zurth, K.; Morelli, G.; Torrea, G.; Guiyoule, A.; Carniel, E. *Yersinia pestis*, the cause of plague, is a recently emerged clone of *Yersinia pseudotuberculosis*. *Proc. Natl. Acad. Sci. U.S.A.* **1999**, *96*, 14043–14048.
(39) Ellison, D. W.; Miller, V. L. Regulation of virulence by members of the MarR/SlyA family. *Curr. Opin. Microbiol.* **2006**, *9*, 153–159.
(40) Hong, M.; Fuangthong, M.; Helmann, J. D.; Brennan, R. G. Structure of an OhrR—*ohrA* operator complex reveals the DNA binding mechanism of the MarR family. *Mol. Cell* **2005**, *20*, 131–141.
(41) Clinical and Laboratory Standards Institute. *Methods for Dilution Antimicrobial Susceptibility Tests for Bacteria that Grow Aerobically; Approved Standard, M07-A7*, 7th ed.; Clinical and Laboratory Standards Institute: Wayne, PA, **2006**.